ISSN 1063-7788, Physics of Atomic Nuclei, 2024, Vol. 87, No. 4, pp. 541–547. © The Author(s), 2024. This article is an open access publication.

NUCLEI
Nuclei

Spin-Dipole Strengths and Neutron Skin Thickness of ^{90}Zr, ^{132}Sn, ^{208}Pb

I. N. Borzov[1),2)*] and S. V. Tolokonnikov[1),3)]**

Received January 12, 2024; revised January 12, 2024; accepted January 22, 2024

Abstract—The strength distributions of charge exchange spin-dipole excitations are calculated in the continuum quasiparticle random-phase approximation based on the Fayans density functional with modified isovector part. An impact of the isovector parameter h_2^- of the DF3-f functional on the strength functions of charge-exchange spin-dipole excitations (0^-, 1^-, 2^-) are studied for ^{208}Pb, ^{132}Sn and ^{90}Zr. The sum rules are calculated using both ground state radii and direct integration of the total SD strength distributions. A comparison with the experimental SD sum rule in ^{90}Zr gives one a possibility to check previously estimated h_2^- values which described well the recent combined estimate for ΔR_{np} in ^{208}Pb and corresponding equation of state parameters – symmetry energy $J_0 = J(\rho_0)$ and a slope parameter $L_0 = L(\rho_0)$.

DOI: 10.1134/S1063778824700480

1. INTRODUCTION

The equation of state of isospin asymmetric nuclear matter determines the essential physical properties of nuclear systems from very neutron-rich nuclei to neutron stars [1]. As the neutron–proton asymmetry and symmetry energy of nuclei increases, the neutron and proton density distributions differ more substantially leading to formation of the neutron skins or neutron halos in neutron-rich nuclei.

The neutron skin thickness, defined as the difference between the root mean square (rms) radii of the proton and neutron distributions constrains the nuclear matter and neutron matter equations of state. The density dependence of the symmetry energy symmetry energy $J_0 = J(\rho_0)$ and a slope parameter $L_0 = L(\rho_0)$ in the vicinity of the nuclear equilibrium density ρ_0 correlates with the neutron-skin thickness which is the difference of neutron and proton rms radii $\Delta R_{np} = \sqrt{\langle r^2\rangle_n} - \sqrt{\langle r^2\rangle_p}$. This is a result of competition between surface-tension and symmetry-energy effects. The uncertainty in these quantities remains high at the present time mostly due to the poorly constrained isovector components of the *NN*-interaction. This influences the predictions of both nuclear properties and reliability of simulation of core-collapse supernovae and neutron stars.

Many of observables determined by isovector part of nuclear energy density functional are sensitive to the stiffness of symmetry energy and neutron skin thickness. An indirect information on ΔR_{np} can be obtained from analysis of the energies of pygmy- and giant dipole resonances, the energy differences between the Gamow–Teller and isobar-analog (anti-analog) resonances [2] and the dipole polarizability of very neutron-rich nuclei [3]. Interestingly enough, the neutron skin thickness is correlated with the product of the electric dipole polarizability and the symmetry energy at saturation density [4].

Several experimental techniques have been effectively applied for derivation of a neutron skin in neutron-rich nuclei since numerous experiments on excitation of isovector giant dipole resonances in (α,α)-scattering. The DWIA analysis of proton elastic scattering on ^{90}Zr [5] at 800 MeV gave ΔR_{np}= 0.09 ± 0.07 fm. Analysis of antiprotonic x-rays scattering on different targets up to ^{238}U resulted in a (model dependent) conclusion that neutron skin thickness of ^{90}Zr equals $\Delta R_{np} = 0.09 \pm 0.02$ fm [6]. An outstanding effort has been undertaken to find the neutron skins of ^{208}Pb and ^{48}Ca from parity-violating electron scattering on ^{208}Pb (PREX-II [7]) and ^{48}Ca (CREX [8]).

In our previous study [9], we have extended the Fayans energy density functional varying its previously unused isovector parameter h_2^- with an additional condition for the upper limit on the energy of the

[1)]National Research Centre "Kurchatov Institute", Moscow, Russia.
[2)]Bogolubov Laboratory of Theoretical Physics, Joint Institute of Nuclear Research, Dubna, Russia.
[3)]Moscow Institute of Physics and Technology (National Research University), Dolgoprudny, Russia.
*E-mail: Borzov_IN@nrcki.ru
**E-mail: Tolokonnikov_SV@nrcki.ru

GDR maximum in the ^{208}Pb nucleus. At the same time, the quality of the previous fit to nuclear densities, nuclear masses, single-particle levels and charge radii was preserved. It was shown that the neutron-skin thickness ΔR_{np} in ^{48}Ca and in ^{208}Pb from the latest combined estimations [10] can be described in a rather narrow interval of $h_2^- = 1.0-1.5$ leading to the estimate of EOS parameters $J_0 = 29.2 \pm 2.6$ MeV, $L_0 = 53.3 \pm 28.2$ MeV.

In the present work we study an impact of the isovector parameter h_2^- of the DF3-f functional on the strength functions of charge-exchange spin-dipole (SD) excitations and corresponding non-energy weighted sum-rules. For the reference ^{208}Pb nucleus, the charge exchange spin-dipole strength functions were reconstructed from the differential cross sections of ^{208}Pb(p, n)^{208}Bi reaction with the polarized protons [11]. The ^{208}Pb(n, p)^{208}Tl reaction cross section has not been fixed yet and the sum rule value is not known. Thus, one has to look for the charge exchange reactions experiments ^{90}Zr(p, n)^{90}Nb and ^{90}Zr(n, p)^{90}Y at 296 MeV [12, 13] in which the SD strength distributions were measured and multipole decomposition analysis [14] lead to the value of sum rule $\Delta S = S_- - S_+ = 147 \pm 13$ fm^2. A comparison with the experimental sum rule in ^{90}Zr gives us yet additional option for estimating the values of ΔR_{np} and corresponding EOS parameters $J(\rho_0)$ and $L(\rho_0)$.

2. THEORY BACKGROUND

The ground state properties are described selfconsistently within the new version of the Fayans energy density functional DF3-f, proposed in [15] to describe isobar-analog resonance (IAR). Then in addition to the screening of the exchange Coulomb term due to the Coulomb–nucleus interaction [15], the h_2^- parameter of isovector part of the functional is activated in the range obtained in [9] from the constraints imposed by nuclear matter EOS:

$$E(\rho,\delta)/A = \mathcal{E}(\rho_p,\rho_n)/\rho, \tag{1}$$

$$\begin{aligned} &E(\rho,\delta)/A \\ &= \varepsilon_{0\mathrm{F}}\left\{\frac{3}{10}\left(\frac{\rho}{\rho_0}\right)^{2/3}\left[(1-\delta)^{5/3}+(1+\delta)^{5/3}\right]\right. \\ &\quad + \frac{1}{3}a_+\frac{1-h_1^+(\rho/\rho_0)^\sigma}{1+h_2^+(\rho/\rho_0)^\sigma}\left(\frac{\rho}{\rho_0}\right) \\ &\quad \left. + \frac{1}{3}a_-\frac{1-h_1^-(\rho/\rho_0)}{1+h_2^-(\rho/\rho_0)}\left(\frac{\rho}{\rho_0}\right)\delta^2\right\}. \end{aligned} \tag{2}$$

Here $\varepsilon_{\mathrm{F}}^p$, ρ_p, $\varepsilon_{\mathrm{F}}^n$, ρ_n are the Fermi energy and proton (neutron) density, $\rho = \rho_p + \rho_n$, $\delta = ((\rho_p - \rho_n))/\rho$—the asymmetry parameter, $\rho_0 = 2k_{\mathrm{F}}^{0\,3}/3\pi^2 = 0.164(7)\mathrm{fm}^{-3}$—equilibrium density of symmetrical nuclear matter, $\hbar k_{\mathrm{F}}^0$ is the Fermi momentum of nucleons of one type of particle, $a^{+,-}$ and h_1^+, h_2^- are dimensionless parameters determined from comparison with experimental data on ground states; for the DF3-a functional, the value $\sigma = 1$ is used, $C_0 = (dn/\varepsilon_{\mathrm{F}})^{-1} = 4\varepsilon_{0\mathrm{F}}/3\rho_0$—the inverse density of states of nucleons of the same type on the Fermi surface at the equilibrium point of symmetric matter. The EOS for pure neutron matter corresponds to the value of the isospin asymmetry parameter $\delta = 1$. Starting from the DF3-f functional, for each h_2^- value we calculate the corresponding neutron and proton rms radii, ΔR_{np} values and corresponding EOS parameters $J(\rho_0)$ and $L(\rho_0)$.

For the strength functions of spin–isospin SD excitations, we use the continuum quasiparticle random-phase approximation (CQRPA). As in [16], the resulting DF3-f + CQRPA model uses the effective approximation. The characteristics of the ground states are described completely self-consistently with the Fayans functional DF3-f [15]. One can neglect the spin components in the EDF. This causes a relatively small error in the binding energies (≈100 keV) [17]. Therefore, the spin–isospin effective interaction in the particle-hole channel (ph) is introduced independently. It has a form of the Landau–Migdal contact NN interaction in the particle-hole channel $\mathcal{F}_0$ supplemented by a π-meson and ρ-meson exchanges modified by the nuclear medium [16] : $\mathcal{F}_{ph} = \mathcal{F}_0 + \mathcal{F}_\pi + \mathcal{F}_\rho$. Here we specify only the central spin–isospin term, which (in momentum representation) reads $\mathcal{F}_0 = C_0 g'(\boldsymbol{\sigma}_1,\boldsymbol{\sigma}_2)(\boldsymbol{\tau}_1,\boldsymbol{\tau}_2)$, where the normalization constant is $C_0 = (dn/\varepsilon_{\mathrm{F}})^{-1} = 300$ MeV fm^{-3}, and $g_\prime$ is the "Landau–Migdal constant". Detailed description of the finite-range tensor terms due to the one-pion and one-rho-meson exchanges can be found in our paper [16].

The strength functions of charge-exchange spin-multipole excitations is found, as the response of the nucleus to an external field

$$\hat{V}_0 = \frac{(2L+1)!!}{q^L} j_L(qr) T^M_{JLS}(\mathbf{n},\boldsymbol{\sigma})\tau^\pm, \tag{3}$$

where $\tau^\pm = t_x \pm i t_y$ are the isospin changing operators in beta-plus and beta-minus channels, $\boldsymbol{\sigma}$ is the spin operator and $T^M_{JLS} = [\boldsymbol{\sigma}\otimes\mathbf{Y}_L)]^J_M$ is the spin-angular tensor, q—stands for momentum transfer. For each h_2^- parameter of the DF3-f functional from the trial set $h_2^- = 0.5-3.0$ used in [9] we calculate the

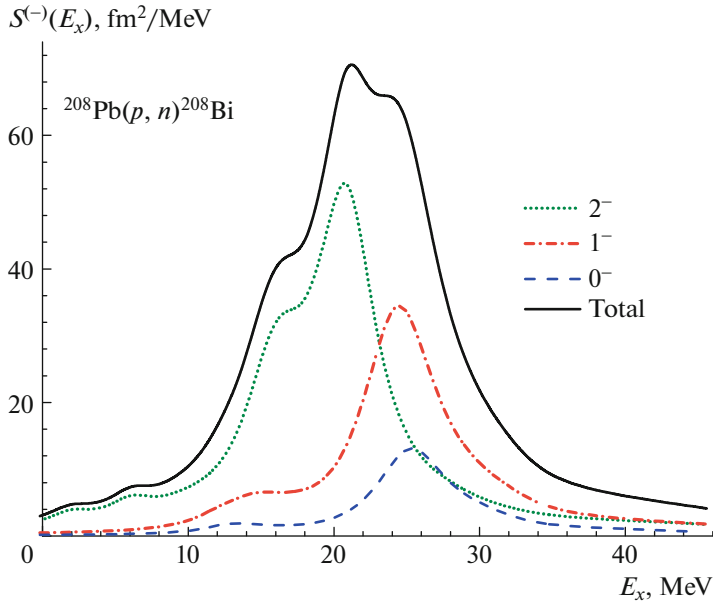

Fig. 1. Strength functions of 0^- (in blue), 1^- (red) and 2^- (green) excitations in ^{208}Pb(p, n)^{208}Bi and the total strength function (full line). Calculation with the DF3-f functional for the $h_2^- = 1.5$.

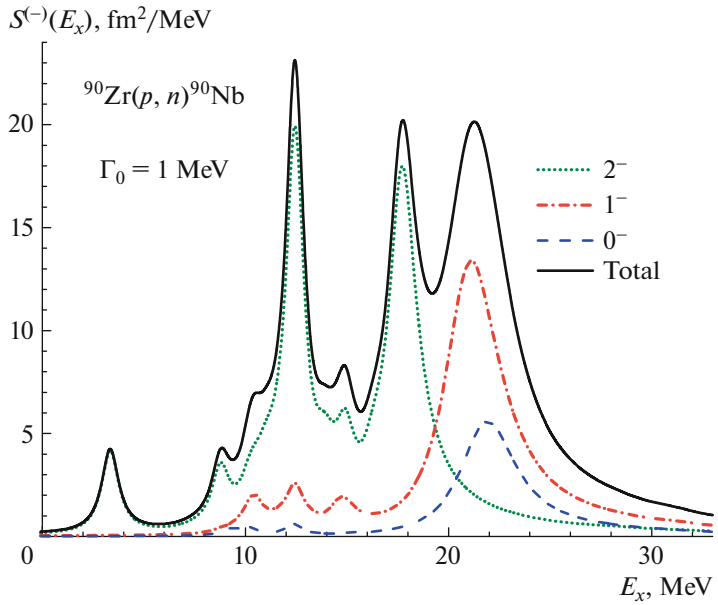

Fig. 2. Strength functions of 0^- (in blue), 1^- (red) and 2^- (green) excitations in ^{90}Zr(p, n)^{90}Nb and total strength function (ful line). Calculation with the DF3-f functional for the $h_2^- = 1.5$.

corresponding SD strength functions for $J^\pi = 0^-$, 1^-, 2^- excitations.

The sum rule for the SD excitations reads

$$\Delta S = \sum_J (S_J^- - S_J^+)$$
$$= \sum_J \frac{2J+1}{4\pi}(N\langle r^2\rangle_n - Z\langle r^2\rangle_p). \qquad (4)$$

As it is seen, the SD sum rule is defined by the neutron and proton mean-square radii. If the SD strength functions were measured, the sum rule, in principle, could be treated as a model-independent (though large experimental uncertainties related to multipole decomposition has to be kept in mind). Naturally, the theoretical sum rule can be obtained by self-consistently calculating the ground state neutron

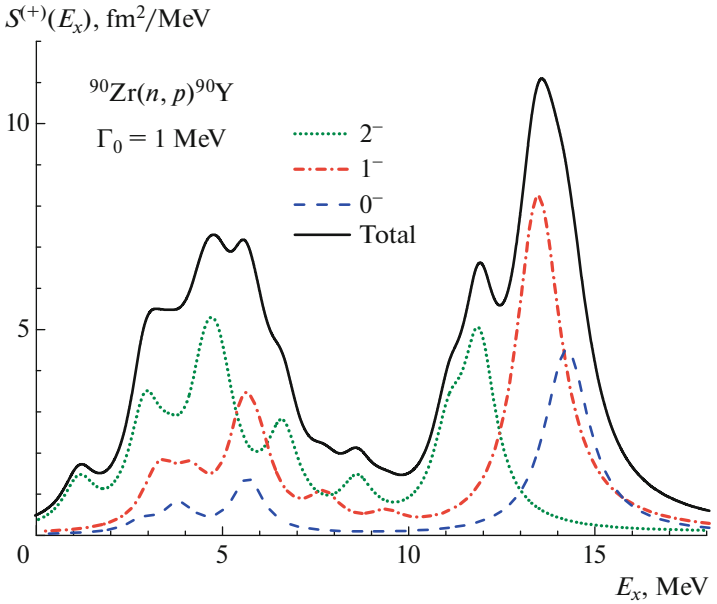

Fig. 3. Strength functions of 0^- (in blue), 1^- (red) and 2^- (green) excitations in ^{90}Zr$(n, p)^{90}$Y and total strength function (ful line). Calculation with the DF3-f functional for the $h_2^- = 1.5$.

and proton radii, or by direct integration of the SD strength function calculated in the DF3-f + CQRPA.

3. CALCULATION DETAILS

In the CQRPA calculations of the strength functions of charge-exchange spin–isospin excitations and the sum rules S^+ and S^- in $\tau^\pm$-channels, besides escape width $\Gamma\uparrow$ associated with the emission of a nucleon into the continuum, we may add the spreading width $\Gamma\downarrow$. In such a way, the fragmentation of excitations associated with complex configurations is taken into account semi-microscopically. In the continuum QRPA framework, the width linearly depends on the excitation energy in the daughter nucleus [17]. In the present calculations, the constant spreading width $\Gamma\downarrow = 1$ MeV is used for the convenience of presentation.

The following values of interaction constants were used in the calculations: $g' = 1.1$, the quenching factors for the SD excitations are $Q_{\rm SD} = (1 - 2\zeta_s)^2$ and for meson–nucleon couplings $f^\pi = -1.45(1 - 2\zeta_s^\pi)^2$ and $f^\rho = 2.64(1 - 2\zeta_s^\rho)^2$ in the normalization $C_0 = 300$ MeV fm^3. The possibility of different quenching for the GTR and SD excitations is still under discussion in the literature. For simplicity, in our calculations all the quenching factors for SD excitations as well as for meson couplings are taken the same as the quenching factor of the GT excitations $Q_{\rm GT} = (g_A/G_A)^2 = (1 - 2\zeta_s)^2$ where, $G_A = 1.27$ being the axial-vector coupling constant of weak interaction, g_A is its medium modified value and $\zeta_s = \zeta_s^\pi = \zeta_s^\rho = 0.08$. Within our approach the value of $Q_{\rm GT}$ was defined from the description of the magnetic moments [18]. It should be noted that the strength constants were determined earlier from calculations of charge-exchange excitations [19]. They do not depend on the mass number A and are kept unchanged in all the calculations.

4. RESULTS

The SD strength distributions are calculated in the CQRPA based on the modified DF3-f functional with activated isovector parameter h_2^-. The low-lying pygmy SD resonances and the giant SD resonances are associated with the parity changing cross-shell transitions with $j = l \pm 1/2 \to j' = l + 1 \pm 1/2$. The calculation in ^{208}Pb, performed without taking into account the quasiparticle–phonon interaction gives for $h_2^- = 1.5$ the maximum energy of total SD strength distribution which is about 1.0 MeV higher than the experimental one (Fig. 1). In Table 1, the sum rule for SD excitations is found a) from the formula (2) using the self-consistently calculated radii and b) by integration of total CQRPA strength functions in beta-minus and beta-plus channels for ^{132}Sn and ^{208}Pb at $h_2^- = 1.5$ and 3.0. For ^{208}Pb, the S^- component of the sum rule (2) in our calculation is up to 1097.4 fm^2 for the energy $E_x < 50$ MeV. Notice that within the same model [15] and for $h_2^- = 1.5$ an exhaustion of the GT sum rule $3(N - Z)$ in ^{208}Pb is 13% for the energy range including pygmy

Table 1. Spin-dipole sum-rule values, proton and neutron rms radii, and thickness of the neutron skin of ^{132}Sn and ^{208}Pb

	^{132}Sn, $h_2^- = 1.5$	^{132}Sn, $h_2^- = 3.0$	^{208}Pb, $h_2^- = 1.5$	^{208}Pb, $h_2^- = 3.0$
$S_- - S_+$ (g.s.)	639.7	608.0	1097.4	1069.5
$S_- - S_+$ (calc.)	617.7	604.2	1069.6	1044.5
$\sqrt{\langle r\rangle_p^2}$ (g.s.)	4.645	4.656	5.441	5.445
$\sqrt{\langle r\rangle_n^2}$ (g.s.)	4.879	4.855	5.606	5.581
$\Delta R_{\rm ch}$ (g.s.)	0.234	0.199	0.165	0.136

Table 2. Spin-dipole sum-rule values, proton and neutron rms radii, and thickness of the neutron skin of ^{90}Zr

h_2^-	0	0.5	1.0	2.0	3.0
$\sqrt{\langle r\rangle_n^2}$ (g.s.)	4.273	4.267	4.262	4.254	4.250
$\sqrt{\langle r\rangle_p^2}$ (g.s.)	4.173	4.176	4.179	4.183	4.186
ΔR_{np} (g.s.)	0.100	0.091	0.083	0.071	0.064
$\sqrt{\langle r\rangle_{\rm ch}^2}$ (g.s.)	4.238	4.241	4.243	4.248	4.251
$S_- - S_+$ (g.s.)	154.96	152.41	150.17	146.77	144.83
$S_- - S_+$ (calc.)	152.46	150.02	148.14	144.88	142.98

resonances, and 62% up to the energy $E_x = 30$ MeV (experimental value $S^-(E_x < 25\ \text{MeV}) = (64 \pm 5)\%$ [20, 21]).

The calculated strength functions of $J^\pi = 0^-, 1^-$ and 2^- excitations in ^{90}Zr(p, n)^{90}Nb reaction, as well as the total spin-dipole strength function are shown in Fig. 2. The position of the peak in total experimental SD strength distribution at the excitation energy $E_x = 20$ MeV is described. The DF3-f + CQRPA calculation predicts a splitting of the SD strength in this region due to 0^- and 1^- excitations. The pygmy-resonance components of the total SD strength distribution at 2 and 12 MeV are mostly due to 2^- excitations. The calculated strength functions of $J^\pi = 0^-, 1^-$ and 2^- excitations in ^{90}Zr(n, p)^{90}Y channel and the total strength function are shown at Fig. 3. The theoretical total experimental SD strength distribution has a pygmy-resonance peak at the excitation energies of $E_x = 5$ MeV and the main resonance peak at 13–14 MeV both having a complicated composition with dominance of 1^- and 2^- excitations. The experimental distribution is rather structureless. Description of the widths in total SD strength function needs some assumptions on the energy dependence of the widths of individual excitations (see e.g. [17, 22]).

As can be seen, the sum rule values corresponding to the same h_2^- are very close to each other. Figure 4 shows the dependence of the sum rule for SD excitations (calculated by direct integration of total CQRPA strength functions) on the the h_2^- parameter and ΔR_{np} value. The experimental value of $\Delta S = 147 \pm 13$ fm^2 [14] is described by $h_2^- = 1.5$ which correspond to $\Delta R_{np} = 0.08 \pm 0.03$ fm close to the results of the experiments on proton elastic scattering [5] and antiprotons annihilation [6].

5. CONCLUSIONS

The spin-dipole excitations strength distributions, neutron skins and parameters of nuclear equation of state are studied for ^{208}Pb, ^{132}Sn and ^{90}Zr within the Fayans density functional with modified isovector part. We investigate an impact of the isovector parameter h_2^- of the DF3-f functional on the strength functions of charge-exchange spin-dipole excitations ($0^-, 1^-, 2^-$). The position of the main peak in total experimental SD strength distribution in ^{90}Zr at the excitation energy $E_x = 20$ MeV is reasonably well described, though the calculation predicts its splitting due to the shift of the 0^- and 1^- excitations maxima.

A good correspondence is observed between the experimental and theoretical non-energy weighted sum-rules calculated for different h_2^- values both by using the g.s. neutron and proton radii and by direct integration of the strength functions. The interval of

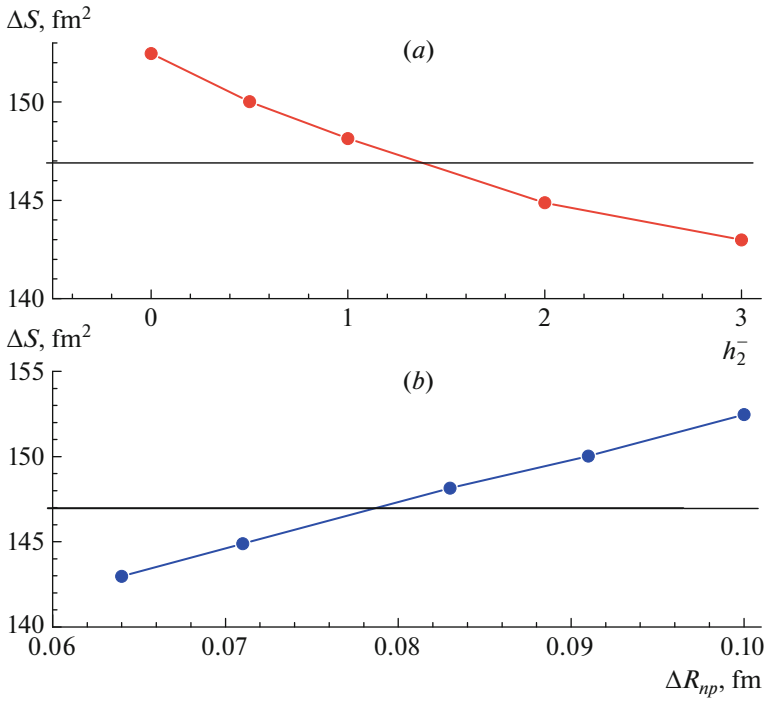

Fig. 4. The total sum rule for SD excitations calculated by integration of total CQRPA strength functions in beta-minus and beta-plus channels. Their dependence is shown on the the h_2^- parameter (upper part) and ΔR_{np} (bottom). The experimental value of $\Delta S = 147 \pm 13$ fm^2 [14] is also shown.

$h_2^- = 1.0{-}1.5$ (Table 2) describing the experimental SD sum rule $\Delta S = 147 \pm 13$ fm^2 [14] and the "experimental" ^{90}Zr neutron skin $\Delta R_{np}(^{90}\text{Zr}) = 0.08 \pm 0.03$ fm [5] and $\Delta R_{np} = 0.09 \pm 0.02$ fm [6] is close to the results obtained in [24] and to the interval found in our paper [9]. The latter was shown to provide a good description of the $\Delta R_{np}(^{208}\text{Pb}) = 0.18 \pm 0.004$ fm and corresponding EOS parameters $J_0 = 29.2 \pm 2.6$ MeV, $L_0 = 53.3 \pm 28.2$ MeV derived in [10] from a combined analysis of the values of the "neutron skin" ΔR_{np} of ^{208}Pb and ^{48}Ca nuclei from the PREX-II, CREX experiments, the results of ab initio calculations of EOS and the properties of the ground states of nuclei, from astrophysical observations and data on the detection of gravitational waves from the merger of binary neutron stars.

New experimental data on the charge-exchange sum rule in a number of neutron-rich isotopes based on a reliable multipole decomposition technique would be desirable, as they can give an additional information on density dependence of symmetry energy.

FUNDING

This work was supported by the Russian Foundation for Basic Research, project no. 21-52-12035.

CONFLICT OF INTEREST

The authors of this work declare that they have no conflicts of interest.

OPEN ACCESS

REFERENCES

1. V. E. Fortov, *Thermodynamics and Equations of State for Matter: From Ideal Gas to Quark-Gluon Plasma* (Fizmatlit, Moscow, 2013; World Scientific, Singapore, 2016).

2. D. Vretenar, N. Paar, T. Nikšić, and P. Ring, Phys. Rev. Lett. **91**, 262502 (2003). https://doi.org/10.1103/physrevlett.91.262502
3. J. Piekarewicz, B. K. Agrawal, G. Colò, W. Nazarewicz, N. Paar, P.-G. Reinhard, X. Roca-Maza, and D. Vretenar, Phys. Rev. C **85**, 41302 (2012). https://doi.org/10.1103/physrevc.85.041302
4. N. E. Solonovich, N. N. Arsenyev, and A. P. Severyukhin, Phys. Part. Nucl. Lett. **19**, 473 (2022). https://doi.org/10.1134/s1547477122050387
5. J. Zenihiro, H. Sakaguchi, T. Murakami, M. Yosoi, Y. Yasuda, S. Terashima, Y. Iwao, H. Takeda, M. Itoh, H. P. Yoshida, and M. Uchida, Phys. Rev. C **82**, 044611 (2010). https://doi.org/10.1103/PhysRevC.82.044611
6. A. Trzcińska, J. Jastrzębski, P. Lubiński, F. J. Hartmann, R. Schmidt, T. Von Egidy, and B. Kłos, Phys. Rev. Lett. **87**, 82501 (2001). https://doi.org/10.1103/physrevlett.87.082501
7. D. Adhikari, H. Albataineh, D. Androic, K. Aniol, D. S. Armstrong, T. Averett, C. Ayerbe Gayoso, S. Barcus, V. Bellini, R. S. Beminiwattha, J. F. Benesch, et al. (PREX Collaboration), Phys. Rev. Lett. **126**, 172502 (2021). https://doi.org/10.1103/PhysRevLett.126.172502
8. D. Adhikari, H. Albataineh, D. Androic, K. A. Aniol, D. S. Armstrong, T. Averett, C. Ayerbe Gayoso, S. K. Barcus, V. Bellini, R. S. Beminiwattha, J. F. Benesch, et al. (CREX Collaboration), Phys. Rev. Lett. **129**, 042501 (2022). https://doi.org/10.1103/PhysRevLett.129.042501
9. I. N. Borzov and S. V. Tolokonnikov, Phys. At. Nucl. **86**, 304 (2023). https://doi.org/10.1134/s1063778823030067
10. R. Essick, P. Landry, A. Schwenk, and I. Tews, Phys. Rev. C **104**, 65804 (2021). https://doi.org/10.1103/physrevc.104.065804
11. T. Wakasa, M. Okamoto, M. Dozono, K. Hatanaka, M. Ichimura, S. Kuroita, Y. Maeda, H. Miyasako, T. Noro, T. Saito, Y. Sakemi, T. Yabe, and K. Yako, AIP Conf. Proc. **85**, 64606 (2012). https://doi.org/10.1063/1.4801675
12. T. Wakasa, H. Sakai, H. Okamura, H. Otsu, S. Fujita, S. Ishida, N. Sakamoto, T. Uesaka, Y. Satou, M. B. Greenfield, and K. Hatanaka, Phys. Rev. C **55**, 2909 (1997). https://doi.org/10.1103/PhysRevC.55.2909
13. K. Yako, H. Sakai, M. B. Greenfield, K. Hatanaka, M. Hatano, J. Kamiya, H. Kato, Y. Kitamura, Y. Maeda, C. L. Morris, H. Okamura, J. Rapaport, T. Saito, Y. Sakemi, K. Sekiguchi, Y. Shimizu, K. Suda, A. Tamii, N. Uchigashima, and T. Wakasa, Phys. Lett. B **615**, 193 (2005). https://doi.org/10.1016/j.physletb.2005.04.032
14. K. Yako, H. Sagawa, and H. Sakai, Phys. Rev. C **74**, 51303 (2006). https://doi.org/10.1103/physrevc.74.051303
15. I. N. Borzov and S. V. Tolokonnikov, Phys. At. Nucl. **82**, 560 (2019). https://doi.org/10.1134/s106377881906005x
16. I. N. Borzov and S. V. Tolokonnikov, Phys. At. Nucl. **86**, 304 (2023). https://doi.org/10.1134/s1063778823030067
17. J. Margueron, S. Goriely, M. Grasso, G. Colò, and H. Sagawa, J. Phys. G: Nucl. Part. Phys. **36**, 125103 (2009). https://doi.org/10.1088/0954-3899/36/12/125103
18. G. F. Bertsch and R. A. Broglia, *Oscillations in Finite Quantum Systems* (Cambridge Univ. Press, Cambridge, 1994).
19. D. J. Horen, C. D. Goodman, C. C. Foster, C. A. Goulding, M. B. Greenfield, J. Rapaport, D. E. Bainum, E. Sugarbaker, T. G. Masterson, F. Petrovich, and W. G. Love, Phys. Lett. B **95**, 27 (1980). https://doi.org/10.1016/0370-2693(80)90391-3
20. I. N. Borzov, E. E. Saperstein, and S. V. Tolokonnikov, Phys. At. Nucl. **71**, 469 (2008). https://doi.org/10.1134/s1063778808030095
21. I. N. Borzov, Phys. Rev. C **67**, 025802 (2003). https://doi.org/10.1103/PhysRevC.67.025802
22. A. Krasznahorkay, H. Akimune, M. Fujiwara, M. N. Harakeh, J. Jänecke, V. A. Rodin, M. H. Urin, and M. Yosoi, Phys. Rev. C **64**, 67302 (2001). https://doi.org/10.1103/physrevc.64.067302
23. A. P. Severyukhin, N. N. Arsenyev, I. N. Borzov, R. G. Nazmitdinov, and S. Åberg, Phys. At. Nucl. **83**, 171 (2020). https://doi.org/10.1134/s106377882002026x
24. Sh.-H. Cheng, J. Wen, L.-G. Cao, and F.-Sh. Zhang, Chin. Phys. C **47**, 024102 (2023). https://doi.org/10.1088/1674-1137/aca38e